Improving Nanosatellite Imaging and Atmospheric Sensing with Adaptive Optics

Anne Marinan*, Kerri Cahoy, Ewan Douglas (MIT)
John Merk (Aurora Flight Sciences)
Ruslan Belikov, Eduardo Bendek (NASA Ames)

7 August 2016

29th Annual AIAA/USU
Conference on Small Satellites

Outline

- **Introduction**
  - **Adaptive Optics overview**
  - **In-space applications**
- Approach: CubeSat Deformable Mirror Demonstration
  - Mission Goals
  - Payload and experiment design
- Flight mission
  - Laboratory validation
  - Status

Introduction – Adaptive Optics

- Adaptive optics correct optical distortions
  - Deformable mirror: actuators change the shape of the mirror surface to match the incoming wavefront

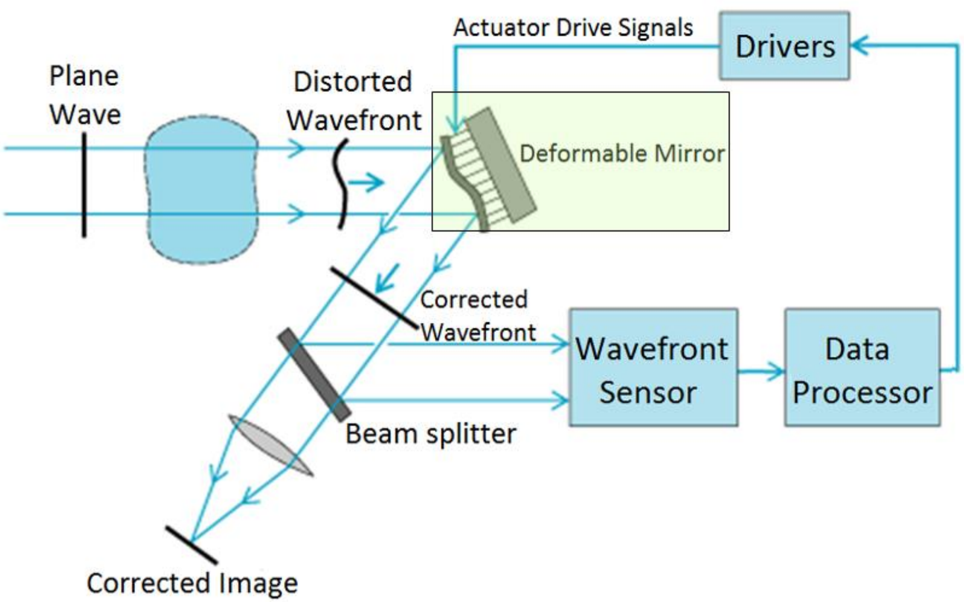

- MEMS deformable mirrors
  - Electrostatic actuators – no hysteresis
  - Smaller size, weight, power, and cost for same number of actuators (compared to piezoelectric or electroceramic)
  - Ideal for use in constrained environment (e.g. space telescope), but have not been space-qualified

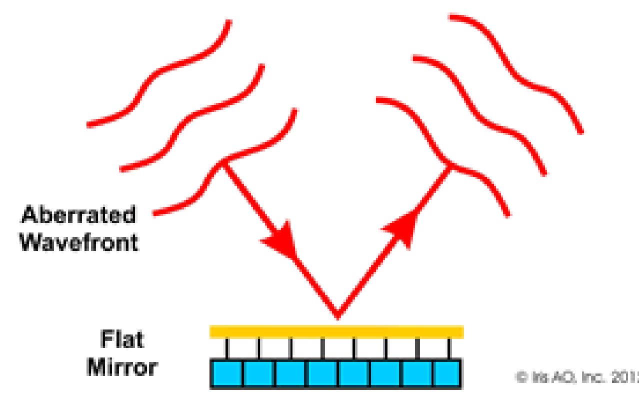

Adaptive Optics Applications in Space

- High-contrast imaging
  - Counteract jitter, thermal gradients, mechanical misalignment, surface roughness
  - <1 Hz timescale
  - More actuators allows for higher spatial frequency correction
  - **Nanosatellites**: validate technology (MEMS DM) for implementation on future space telescopes

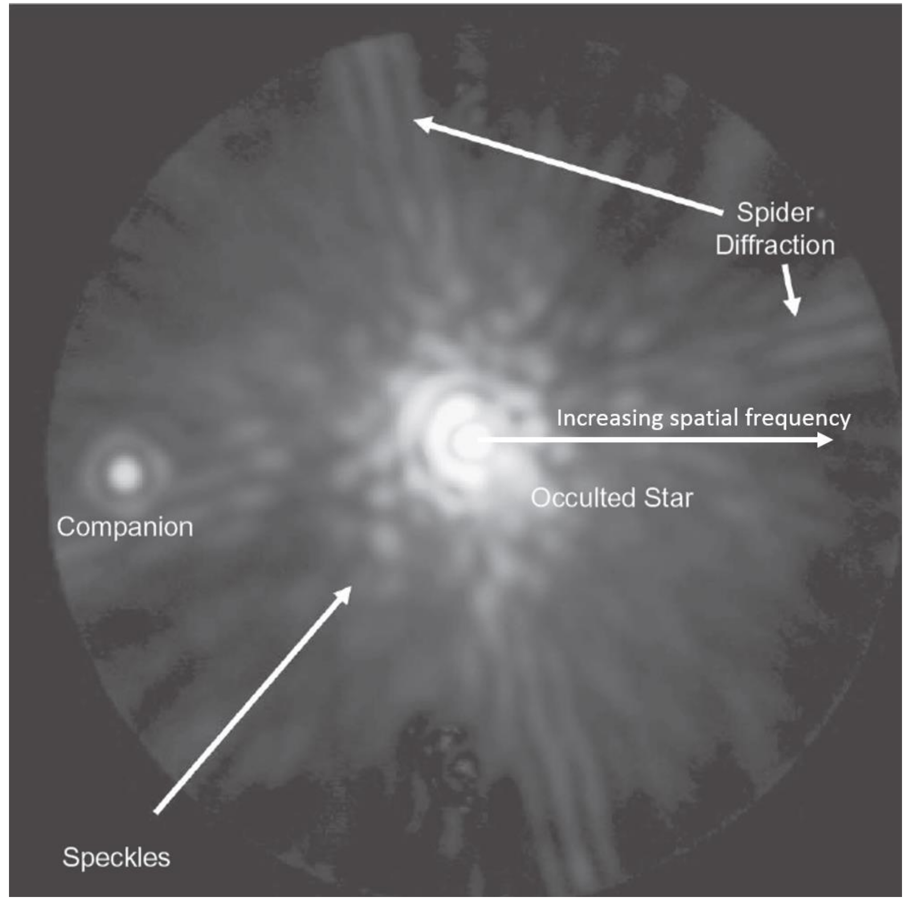

Coronagraph Image Plane
Higher spatial frequency (more actuators) = farther from image center
Traub, Oppenheimer 2010

Adaptive Optics Applications in Space

- Atmospheric sensing with intersatellite optical occultation
  - Correct for scintillation and distortions to sound lower into the atmosphere
  - > 1 kHz timescale
  - **Nanosatellites**: technology validation and measurement platform

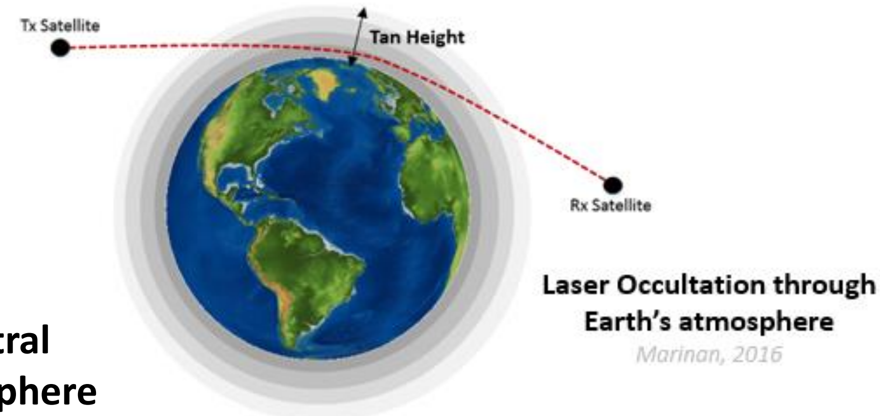

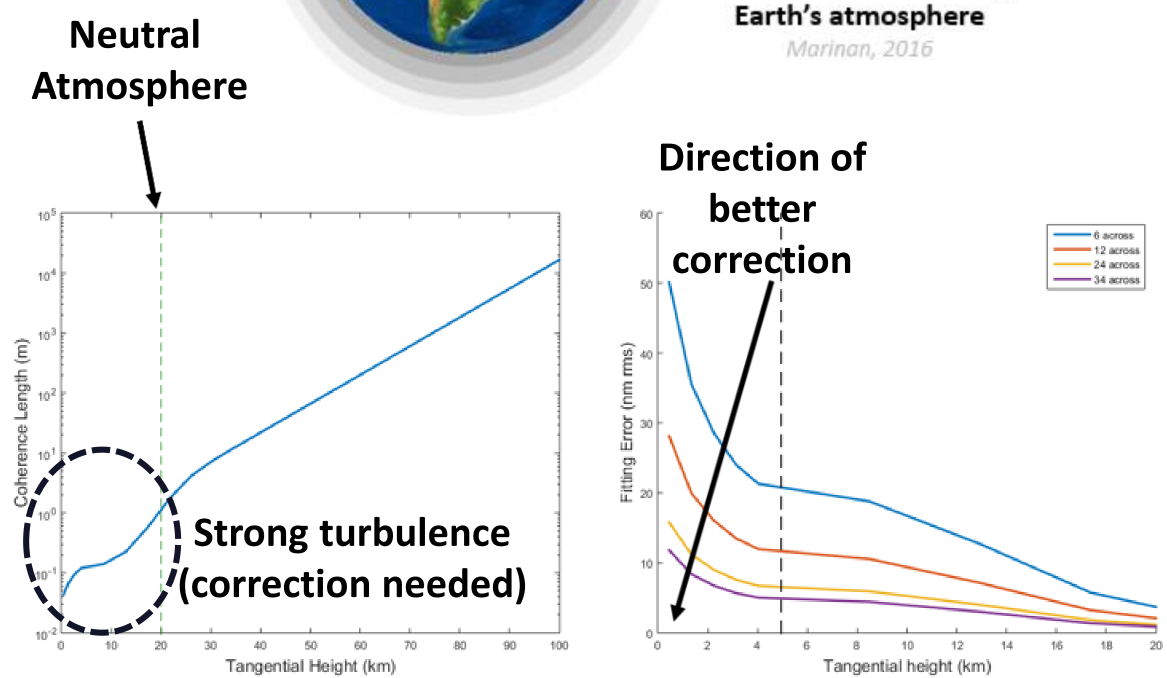

Atmospheric turbulence worse near the surface (left); more actuators allow for better-matched correction (right)

Outline

- Introduction
  - Adaptive Optics overview
  - In-space applications
- **Approach: CubeSat Deformable Mirror Demonstration**
  - **Mission Goals**
  - **Payload and experiment design**
- Flight mission
  - Laboratory validation
  - Status

CubeSat **De**formable **Mi**rror Demonstration

- DeMi Mission Goals:
  - Characterize and calibrate the performance of a MEMS deformable mirror over a long-duration on-orbit mission
    - Measure mirror surface to <100 nm
  - Demonstrate the use of these mirrors as intended for high contrast imaging
    - Correct in situ aberrations to < 100 nm rms
- Baseline orbit: ISS (~404x424 km)
- Target stars: Vega, Arcturis, Sirius, Canopis, Alpha Centauri
  - 5-8 minute orbit-averaged access opportunities

Notional rendering of 6U demonstration CubeSat

Image Credit: Aurora Flight Sciences

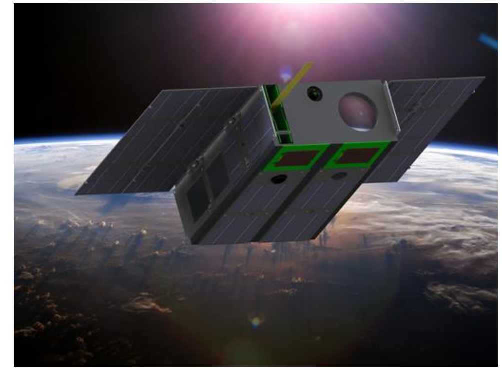

Payload Requirements and Specs

Subsystem	Requirement
Attitude knowledge	0.1 degrees
Attitude stability	<20 arcsec over 1 ms
Power	< 10 W
Datarate	50 kbps
Volume	2U for optics 0.5 – 1U for driver
Mass	< 1.5 kg

DeMi Payload Design

- 2U Optical payload
  - Mirror: BMC Multi (140 actuators)
    - Alternate: Kilo (952 actuators) with custom driver developed by NASA Ames

BMC Mini/Multi Mirror Form Factor

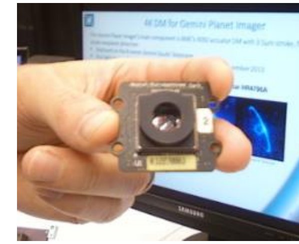

Mirror Characterization Payload Layout
Green: External source
Blue: Internal source
Marinan 2016

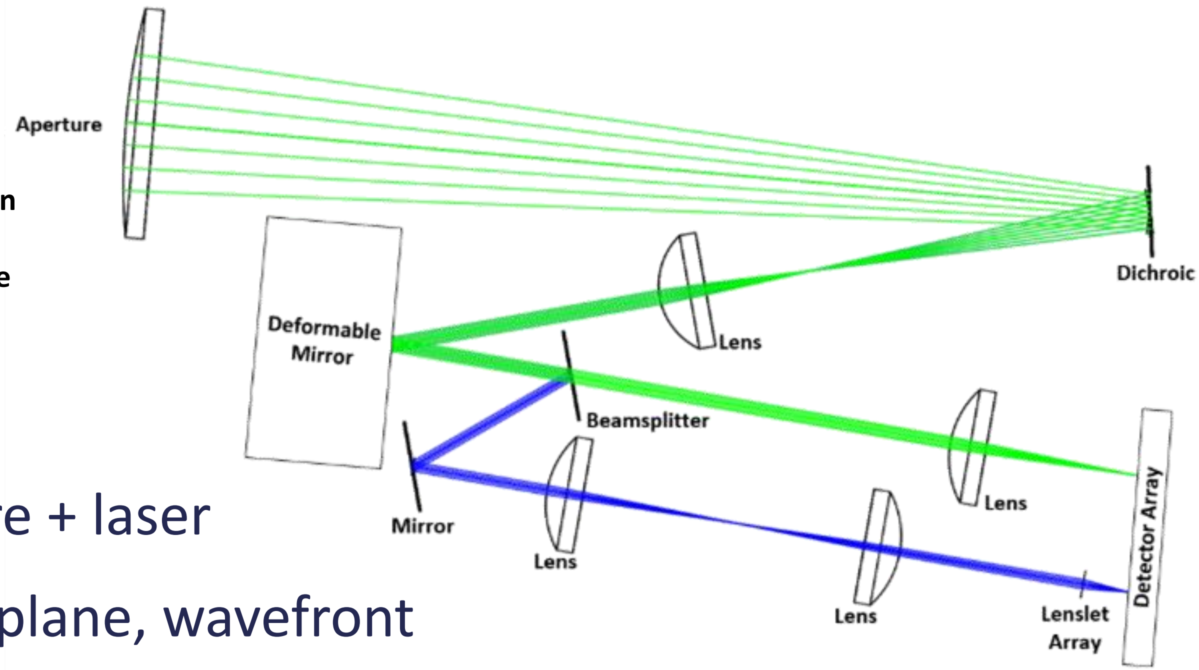

- 2 sources: aperture + laser
- 2 detectors: focal plane, wavefront sensor

DeMi Experiment Architectures

0 – Internal source + wavefront sensor

- Open-loop mirror characterization, closed-loop correction
- Experiment run periodically throughout mission life

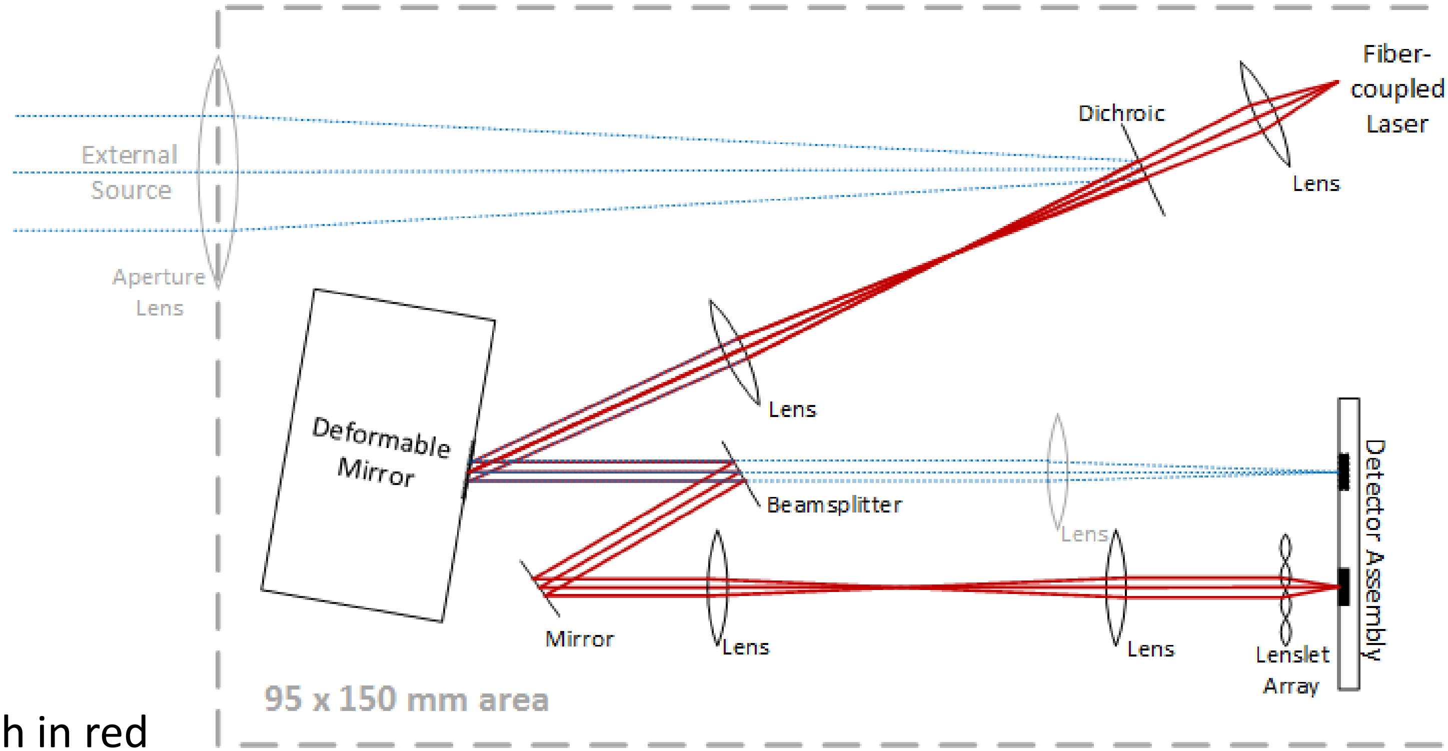

Beampath in red

A. Marinan, MIT

DeMi Experiment Architectures

1 – Internal source + focal plane image

- Closed-loop correction with focal plane sensor
- Experiment run periodically throughout mission life

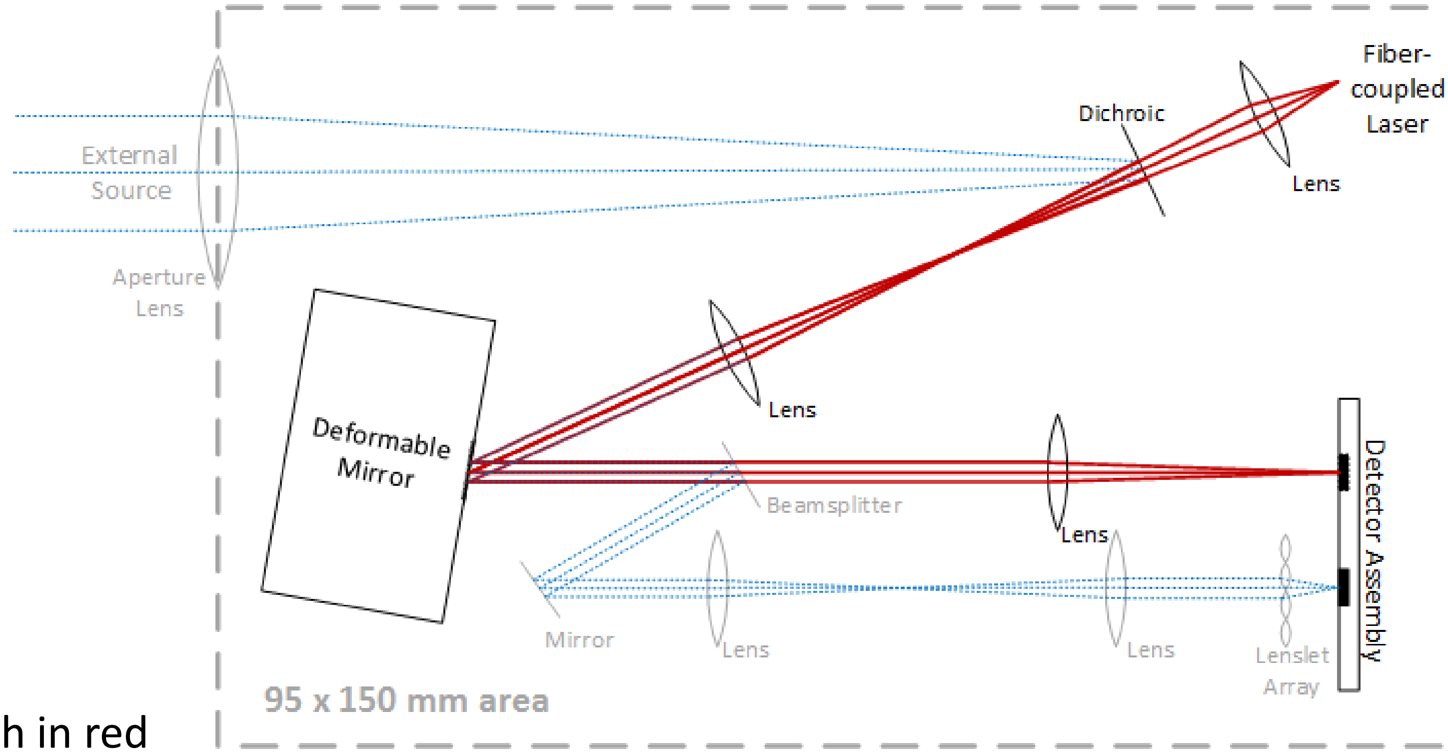

Beampath in red

A. Marinan, MIT

DeMi Experiment Architectures

2 – External object + focal plane image

- Closed-loop image correction with focal plane sensor
- Experiment of opportunity (bright star in view)

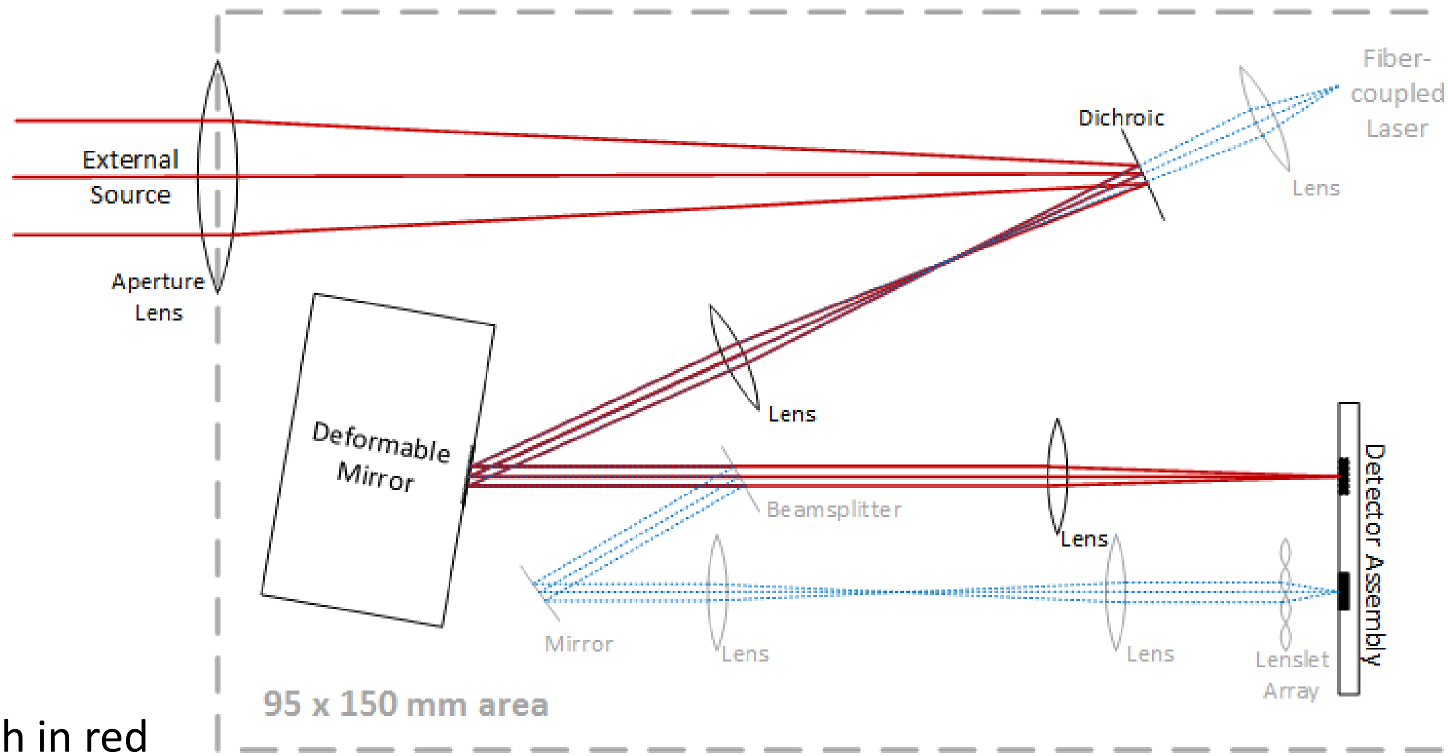

Beampath in red

A. Marinan, MIT

Outline

- Introduction
  - Adaptive Optics overview
  - In-space applications
- Approach: CubeSat Deformable Mirror Demonstration
  - Mission Goals
  - Payload and experiment design
- **Flight mission**
  - **Laboratory validation**
  - **Status**

CubeSat Payload – In-lab Validation

- To-scale optical payload
  - Some modifications for mirror, detector packaging
  - Mini deformable mirror (32 actuators)
- Wavefront reconstruction and control software, drivers written in MATLAB on desktop computer
  - Non-flight configuration
- Overall goal for setup:
  - Verify wavefront sensor measurement precision -> inform performance of payload in LEO
  - Demonstrate closed-loop control

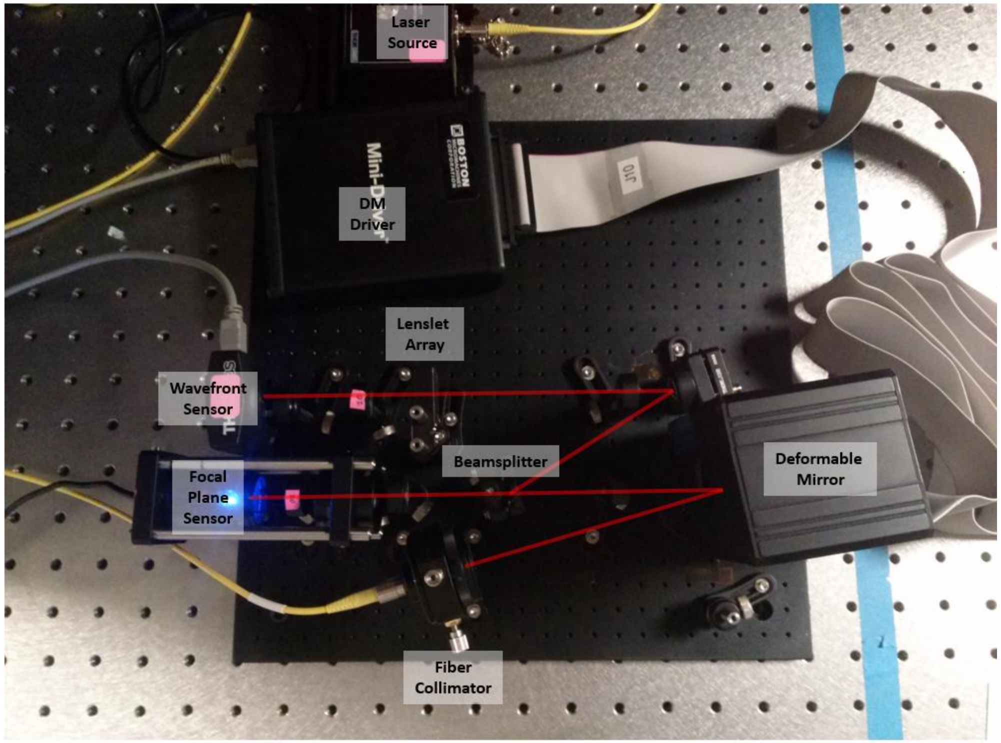

Laboratory hardware setup with key system elements

Marinan, 2016

Open-Loop Laboratory Validation

- Payload wavefront sensor (left) showing behavior consistent with Zygo interferometer measurements (right)
  - Shack Hartmann wavefront sensor, 4 lenslets (samples) per actuator
  - ~80 nm deflection at 20% stroke
  - Noisier than Zygo measurements (less controlled environment, noise in wavefront sensor measurement)

32 phase maps of influence function for each actuator poke
(left) computed with wavefront sensor, (right) from Zygo interferometer
Note: each subplot shows entire mirror surface

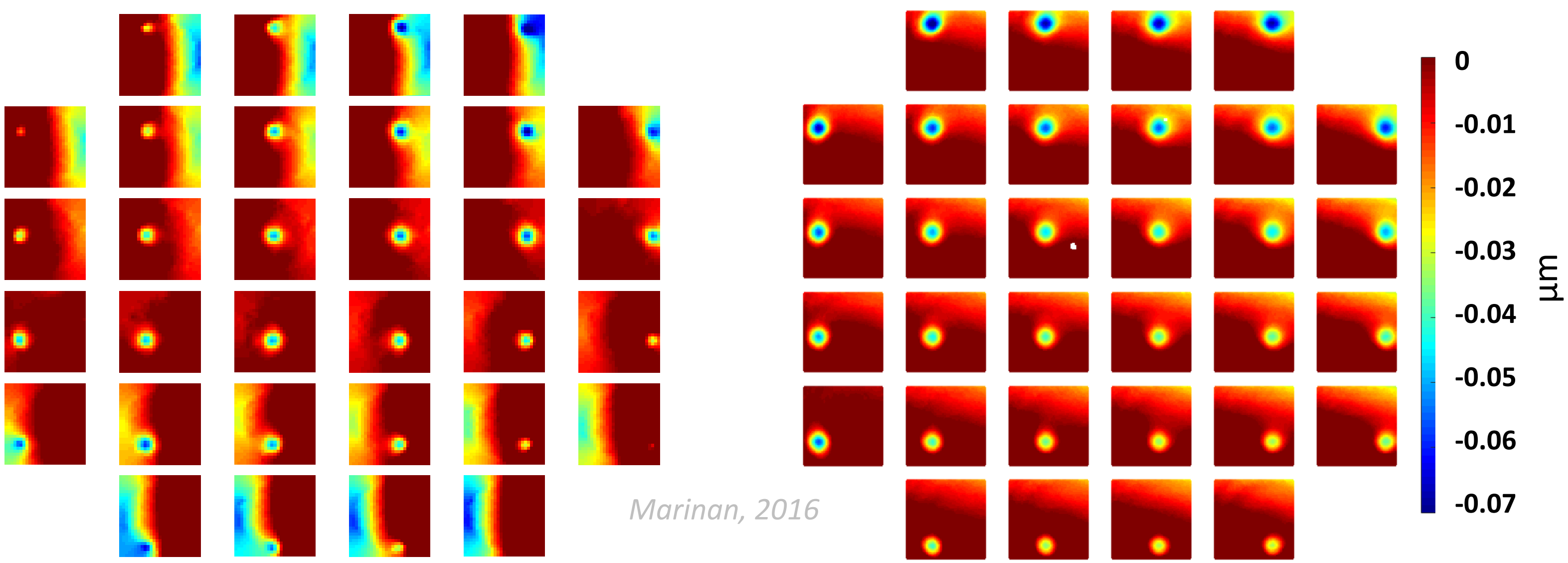

Closed-Loop Laboratory Validation

- Control law implemented
  - Wavefront sensor sending feedback to deformable mirror
  - Image correction (aberration with plastic plate) observed in focal plane
  - Mirror responding as expected, no observed system instabilities
- Slow static correction
  - 2-3 second iterations, converges after ~35 seconds
  - Limited in correction capability (6 actuators across – limited spatial frequency)

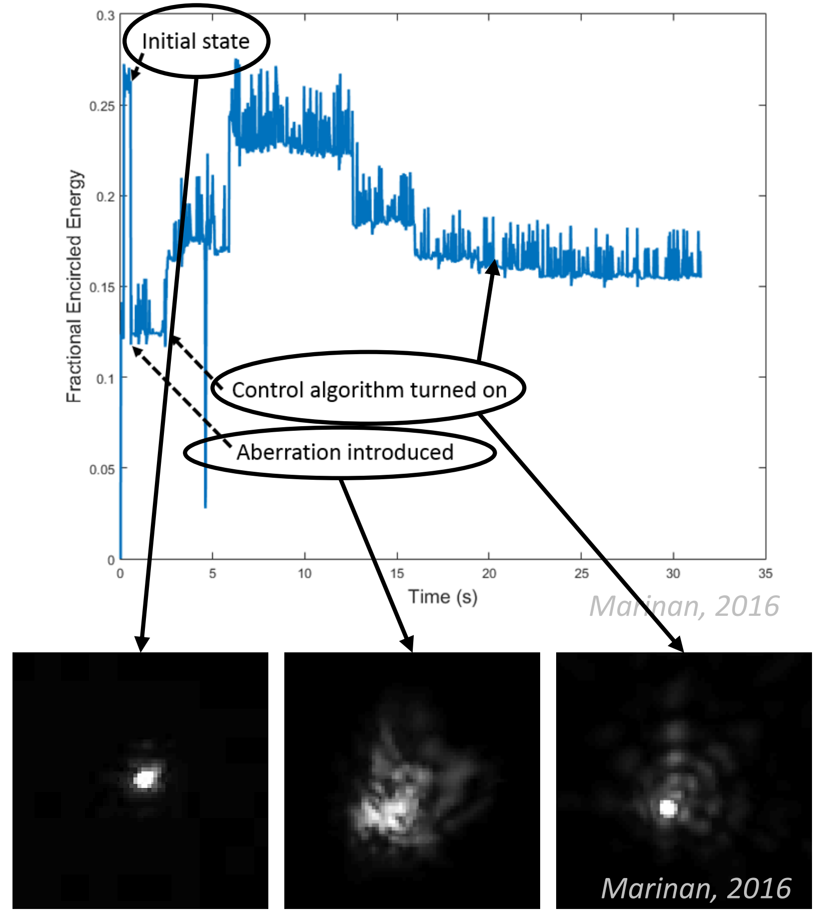

(Left) Initial focal plane image
(Middle) Focal plane image with aberration
(Right) Focal plane image after correction

Flight Mission – Status and Path Forward

- Selected by DARPA for 6U flight demonstration (pending contract negotiations)
  - Collaboration between MIT and Aurora Flight Sciences
- Scale payload design for 140 or 952-actuator mirror
  - Advantages: higher spatial frequency correction authority (coma, spherical, higher-order modes)
- Exploring alternate wavefront sensing algorithms or wavefront/metrology sensors
  - On-orbit updates could enable testing of multiple algorithms
- Flight design and build of supporting optomechanics (look into 3D printing)

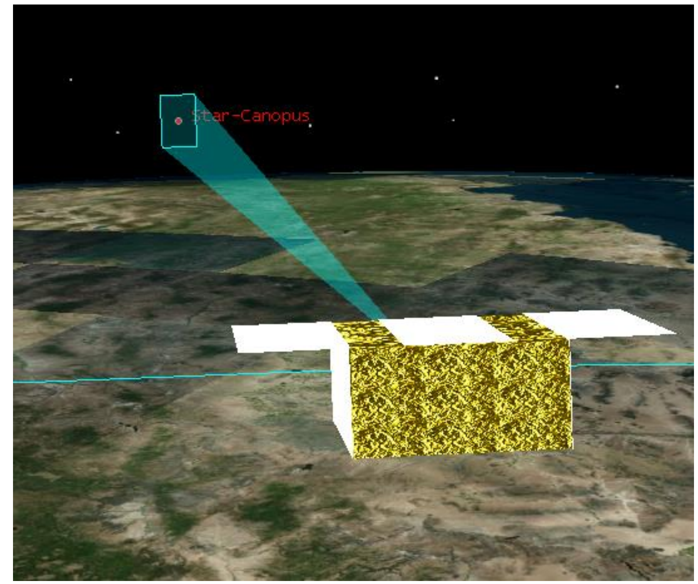

Star-pointing DeMi mission concept illustration

Marinan, 2016

Summary

- Adaptive (active) optics useful for space applications
  - High contrast imaging
  - Atmospheric sensing and characterization
- MEMS deformable mirrors offer promising solution for space-based platforms
  - Low SWaP, high actuator density (high spatial frequency control)
  - Have not been space-qualified
- DeMi: CubeSat Deformable Mirror Demonstration
  - Long-term on orbit characterization of MEMS deformable mirror
  - 6U CubeSat with ~2U optical payload
    - Payload prototyped in laboratory at MIT
  - Flight mission currently being negotiated

Thank you!

This research was sponsored by a NASA Space Technology Research Grant (NNX12AM30H)

References

- [1] H. Heidt, J. Puig-Suari, A. Moore, S. Nakasuka, and R. Twiggs, \Cubesat: A New Generation of Picosatellite for Education and Industry Low-Cost Space Experimentation," in SSC00-V-5, Logan, UT, 2001.
- [2] K. Woellert, P. Ehrenfreund, A. Ricco, and H. Hertzfeld, \Cubesats: Costeffective science and technology platforms for emerging and developing nations," Advances in Space Research, vol. 47, pp. 663{684, 2011.
- [3] Committee on Earth Science and Applications from Space, Earth Science and Applications from Space: National Imperatives for the Next Decade and Beyond, English, 2007.
- [4] M.M. Burlacu and P. Lorenz, \A survey of small satellites domain challenges, applications, and communications issues," ICaST: ICST's Global Community Magazine, 2010.
- [5] A. Petro, Small spacecraft technology, 2012. [Online]. Available: http://www. nasa . gov / offices / oct / crosscutting _ capability / edison / smallsat _tech.html.
- [6] Saint Louis University, CubeSat Database. [Online]. Available: http://sites. google.com/a/slu.edu/swartwout/home/cubesat- database (visited on 11/21/2015).
- [7] M. Swartwout, \The First One Hundred CubeSats: A Statistical Look," Journal of Small Satellites, vol. 2, no. 2, pp. 213{233, 2013.
- [8] E. Hand, \Startup Lifto: How ocks of small, cheap satellites, hatched in Silicon Valley, will constantly monitor a changing Earth," Science, pp. 172-177, Apr. 2015.
- [9] Anna Heiney and Brian Dunbar, About ELaNa: Project ELaNa: Launching Education into Space, 2015. [Online]. Available: https://www.nasa.gov/content/about-elana.
- [10] J. Foust, \Spire Raises $40 Million for Weather Satellite Constellation," Jun. 2015. [Online]. Available: http://spacenews.com/spire-raises-40-million-for-weather-satellite-constellation..
- [11] M. D. D. Sta, Small Spacecraft Technology State of the Art, 2014. 95
- [12] D. Selva and D. Krejci, \Review: A Survey and Assessment of the Capabilities of Cubesats for Earth Observation," Acta Astronautica, vol. 74, pp. 50{68, Nov. 2012.
- [13] William Blackwell, \Micromas: First Step Towards a Nanosatellite Constellation for Global Storm Observation," in Proceedings of the 27th Annual AIAA/USU Conference on Small Satellites, Logan, UT, Aug. 2013.
- [14] S. Schweitzer, G. Kirchengast, and V. Proschek, \Atmospheric inuences on infrared-laser signals used for occultation measurements between Low Earth Orbit satellites," Atmospheric Measurement Techniques, vol. 4, pp. 2273{2292, 2011. doi: 10.5194/amt-4-2273-2011.
- [15] William Blackwell, Rebecca Bishop, Kerri Cahoy, Brian Cohen, Clayton Crail, Lidia Cucurull, Pratik Dave, Michael DiLiberto, Neal Erickson, Chad Fish, Shupeng Ho, R. Vincent Leslie, Adam Milstein, and Idahosa Osaretin, \Radiometer Calibration Using Colocated GPS Radio Occultation Measurements," IEEE Transactions on Geoscience and Remote Sensing, vol. 52, no. 10, pp. 6423-6433, 2013. doi: 0.1109/TGRS.2013.2296558.
- [16] Polarcube: An advanced radiometer 3u cubesat. [Online]. Available: http://spacegrant.colorado.edu/allstar-projects/polarcube.
- [17] e. a. W.J. Blackwell, \Microwave radiometer technology acceleration mission (mirata): Advancing weather remote sensing with nanosatellites," in Proceedings of the 28th Annual AIAA/USU Conference on Small Satellites, Logan, UT, 2014.
- [18] W. J. Blackwell and J. Pereira, \New Small Satellite Capabilities for Microwave Atmospheric Remote Sensing: The Earth Observing Nanosatellite-Microwave (EON-MW)," in Proceedings of the 29th Annual AIAA/USU Conference on Small Satellites, Logan, UT, 2015.
- [19] X. Zou, L. Lin, and F. Weng, \Absolute calibration of ATMS upper level temperature sounding channels using GPS RO observations," IEEE Trans. Geo. Remote Sensing, vol. 52, no. 2, pp. 1397{1406, 2014.
- [20] E. Njoku, \Passive microwave remote sensing of the earth from space - a review," in Proceedings of the IEEE, vol. 70, 1982.
- [21] R. Anthes, \Exploring Earth's atmosphere with radio occultation: Contributions to weather, climate and space weather," Atmospheric Measurement Techniques Discussions, vol. 4, pp. 135{212, 2011.
- [22] Rebecca Bishop, David Hinkley, Daniel Stoel, David Ping, Paul Straus, and Timothy Burbaker, \First Results from the GPS Compact Total Electron Content Sensor (CTECS) on the PSSCT-2 Nanosat," Logan, UT, Aug. 2012.
- [23] O. Montenbruck, GNSS Receivers for Space Applications, TU Munchen, May 2008.
- [24] Roy W. Spencer, \The role of passive microwave radiometers in climate monitoring," NASA Space Science and Techology Center, Tech. Rep. 96
- [25] S. T. Brown, S. Desai, W. Lu, and A. Tanner, \On the Long-Term Stability of Microwave Radiometers Using Noise Diodes for Calibration," IEEE Transactions on Geoscience and Remote Sensing, vol. 5, no. 7, pp. 1908{1920, 2007.

References

- [26] K. Cahoy, J.M. Byrne, T. Cordeiro, P. Dav, Z. Decker, A. Kennedy, R. Kingsbury, A. Marinan, W. Marlow, T. Nguyen, S. Shea, W. J. Blackwell, G. Allen, C. Galbraith, V. Leslie, I. Osaretin, M. DiLiberto, P. Klein, M. Shields, E. Thompson, D. Toher, D. Freeman, J. Meyer, and R. Little, \The Microwave Radiometer Technology Acceleration CubeSat (MiRaTA)," in Earth Science Technology Forum, 2015.
- [27] Christina Muth, Paul S. Lee, James C. Shiue, and W. Allan Webb, \Advanced Technology Microwave Sounder on NPOESS and NPP," IEEE, pp. 2454{2458, 2004. doi: 0-7803-8742-2/04.
- [28] E. Robert Kursinski, \The GPS Radio Occultation Concept: Theoretical Performance and Initial Results," English, Doctor of Philosophy, California Institute of Technology, Pasadena, CA, Mar. 1997.
- [29] G.A. Hajj, E. R. Kursinski, L. J. Romans, W. I. Bertiger, and S.S. Leroy, \A technical description of atmospheric sounding by GPS occultation," JASTP, Journal of Atmospheric and Solar-Terrestrial Physics, vol. 64, pp. 451{469, 2002. doi: 1364-6826/02.
- [30] Radiocommunication Sector of ITU, \Attenuation by atmospheric gases," Geneva, Tech. Rep. Recommendation ITU-R P.676-10, Sep. 2013.
- [31] G. Fjeldbo, A. Kliore, and V. R. Eshlemann, \The neutral atmosphere of Venus studied with the Mariner V radio occultation experiments," Journal of Astronomy, vol. 76, no. 2, 123{140, 1971.
- [32] Hajj, G.A. Kursinski, E.R., Schoeld, J. T., Lineld, R. P., and Hardy, K. R., \Observing Earth's atmosphere with radio occultation measurements using the Global Positioning System," Journal of Geophysical Research, vol. 102, no. D19, pp. 23 429{23 465, Oct. 1997. doi: 0148-0227/97/97JD-01569509.00.
- [33] V. Proschek, G. Kirchengast, and S. Schweitzer, \Greenhouse gas proling by infrared-laser and microwave occultation: Retrieval algorithm and demonstration results from end-to-end simulations," Atmospheric Measurement Techniques, vol. 4, pp. 2035{2058, 2011. doi: 10.5194/amt-4-2035-2011.
- [34] Jeremy Harrison, Peter Bernath, and Gottfried Kirchengast, \Spectroscopic requirements for ACCURATE, a microwave and infrared-laser occultation satellite mission," Journal of Quantitative Spectroscopy & Radiative Transfer, vol. 112, pp. 2347{2354, 2011. doi: 10.1016/j.jqsrt.2011.06.003.
- [35] M. Schneider and F. Hase, \Improving spectroscopic line parameters by means of atmospheric spectra: Theory and example for water vapor and solar absorption spectra," Journal of Quantitative Spectroscopy & Radiative Transfer, vol. 110, pp. 1825{1839, 2009. doi: 10.1016/j.jqsrt.2009.04.011. 97
- [36] Wesley Traub and Ben Oppenheimer, \Direct Imaging of Exoplanets," Exoplanets, S. Seager, Ed., pp. 111{156, 2010.
- [37] Paul Bierden, Thomas Bifano, Steven Cornelissen, Jeremy Kasdin, and Marie Levine, \Technology Milestone White Paper: MEMS Deformable Mirror Technology,“ Tech. Rep. JPL Document D-81373, 2013.
- [38] Christopher Mendillo, Supriya Chakrabarti, Timothy Cook, Brian Hicks, and Benjamin Lane, \Flight Demonstration of a milliarcsecond pointing system for direct exoplanet imaging," Applied Optics, vol. 51, no. 29, pp. 7069{7079, Oct. 2012, issn: 1559-128X/12/297069-11.
- [39] Jennifer Roberts, Antonin Bouchez, Rick Burruss, Richard Dekany, Stephen Guiwits, and Mitchell Troy, \Optical Characterization of the PALM-3000 3388-Actuator Deformable Mirror," 2010. [Online]. Available: http://www.oir.caltech.edu/twiki_oir/bin/view/Palomar/Palm3000/WebHome.
- [40] W. Southwell, \Wave-front estimation from wave-front slope measurements,“ English, Journal of Optical Society of America, vol. 70, no. 8, pp. 998{1006, Aug. 1980. doi: 0030-3941/80/081006-04.
- [41] Seng-Whan Bahk, \Highly accurate wavefront reconstruction algorithms overbroad spatial-frequency bandwidth," Optics Express, vol. 19, no. 20, Sep. 2011.
- [42] Johannes Pfund, Norbert Lindlein, and Johannes Schwider, \Misalignment effects of the ShackHartmann sensor," Applied Optics, vol. 37, no. 1, pp. 22{27, Jan. 1998.
- [43] T. Fusco, S. Thomas, M. Nicolle, A. Tokovinin, V. Michau, and G. Rousset, Optimization of Center of Gravity algorithms in a Shack-Hartmann sensor,“ in Proceedings of SPIE, vol. 6272, 2006, pp. 1{11. (visited on 06/09/2014).
- [44] Damien Gratadour, Eric Gendron, and Gerard Rousset, \Symmetrically weighted center of gravity for Shack-Hartmann wavefront sensing on a laser guide star,“ in Proc. SPIE, vol. 7736, 2010.
- [45] Virendra N. Mahajan, \Zernike Circle Polynomials and Optical Aberrations of Systems with Circular Pupils," Supplement to Applied Optics, pp. 8121{8124, Dec. 1994.
- [46] R. J. Noll, \Zernike Polynomials and Atmospheric Turbulence," The Optical Society of America, vol. 66, no. 3, pp. 207{211, Mar. 1976.
- [47] Boston Micromachines Corporation, Mini-dm Specication Sheet, 2014. [Online]. Available: http://www.bmc.bostonmicromachines.com/pdf/Mini-DM.pdf.
- [48] Zygo Corporation, Verire Laser Interferometers, 2010. [Online]. Available:http://www.zygo.com/met/interferometers/verifire/verifire_br.pdf.
- [49] ||, Verire QPZ Specication, 2014. [Online]. Available: http://www.zygo.com/met/interferometers/verifire/qpz/Verifire_QPZ_Specs.pdf.
- [50] ||, MetroPro Reference Guide, version 9.0, 2011.98

Backup Slides

Introduction – Nanosatellite Science Applications

- Nanosatellites (CubeSats) for Atmospheric Sounding and Characterization
  - Science platform
  - Technology development platform
  - Advantages: low cost, high risk tolerance, fast development, distributed system architecture
  - Challenges: tight constraints in volume, mass, power, pointing, data downlink
- ***Want to develop methods to improve atmospheric sensing using nanosatellites in both science and technology development applications***

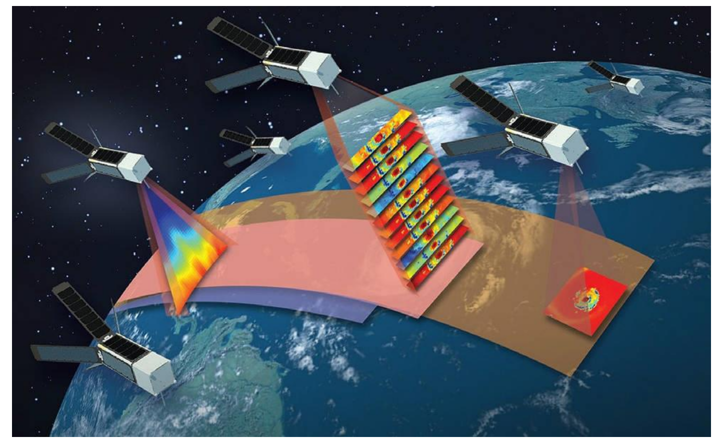

TROPICS Nanosatellite weather sensing constellation

Image credit: MIT LL

Atmospheric Spectroscopy - Occultations

- Transit/Occultations

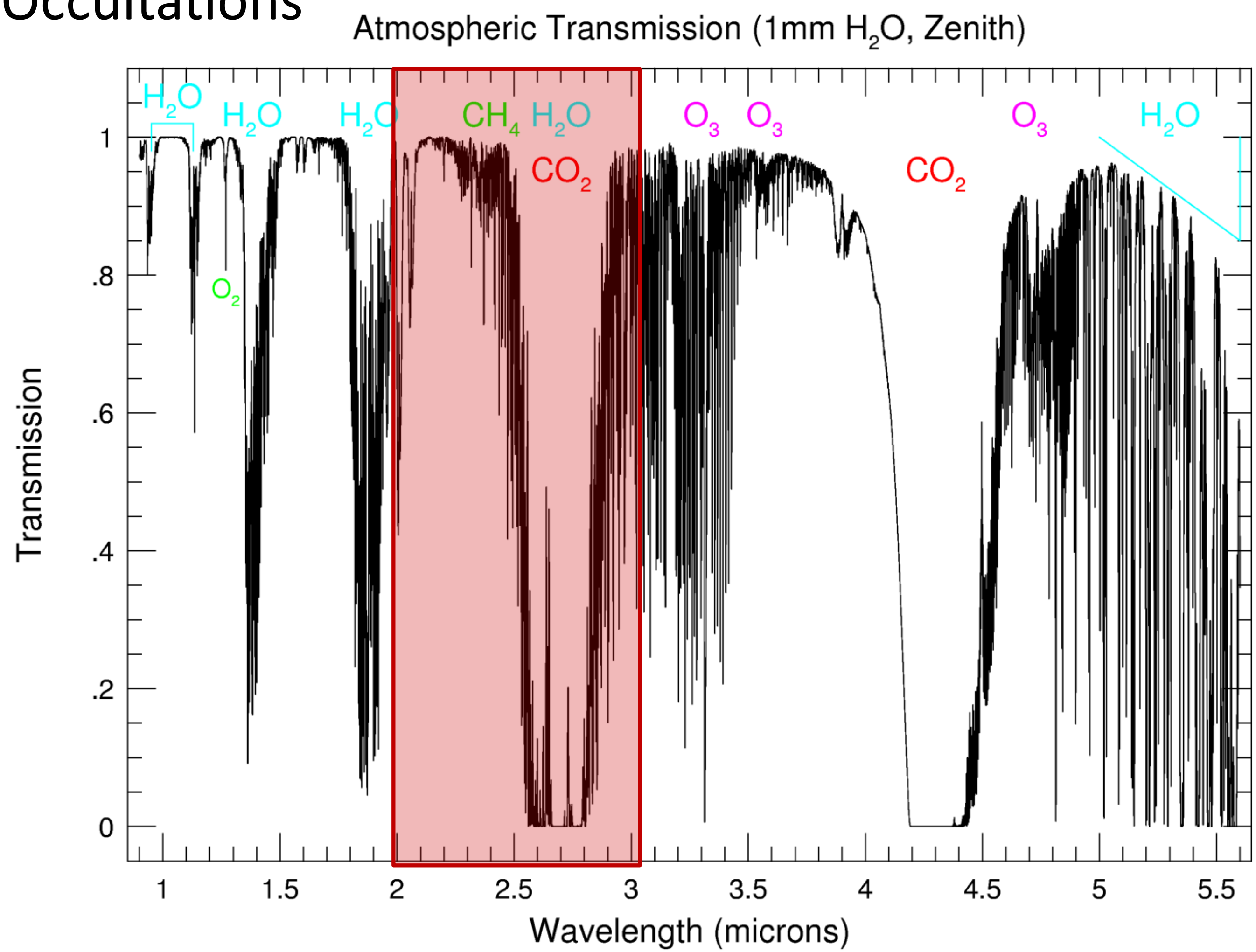

www.astronomy.ohiostate.edu

Occultation Concept

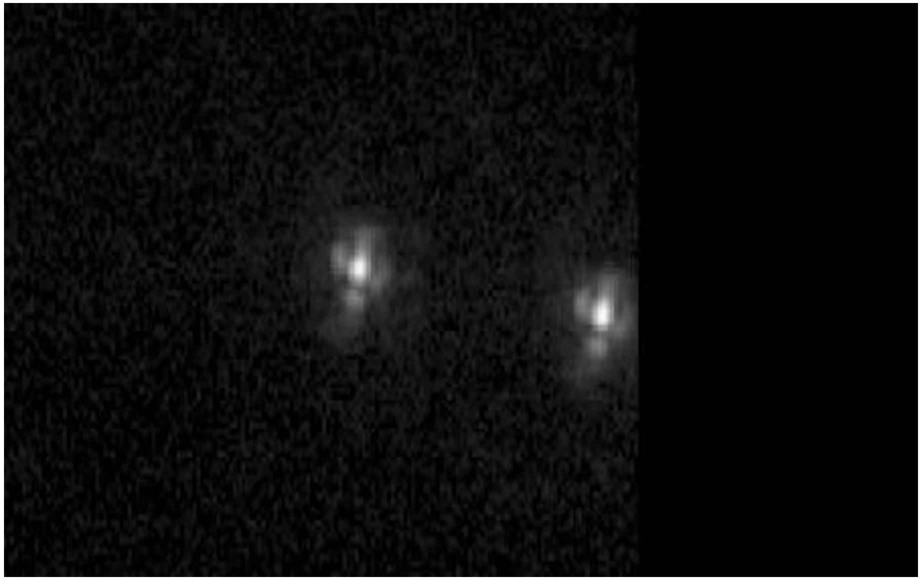

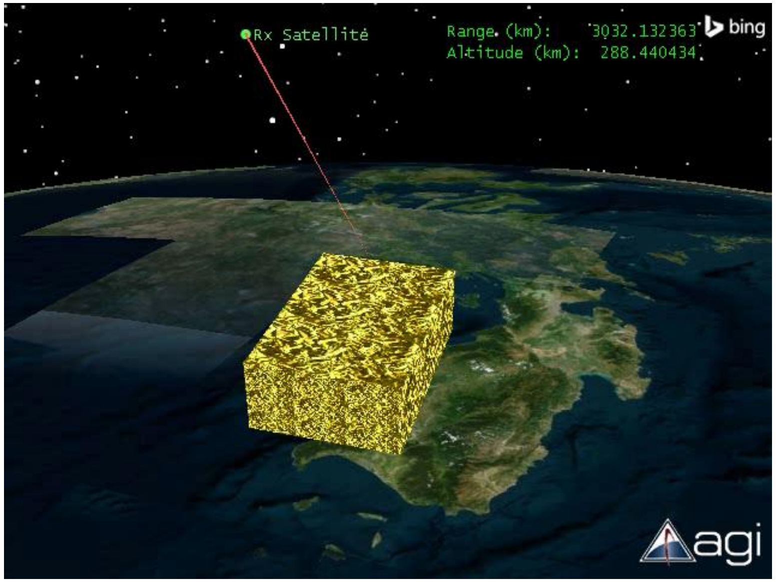

- Titan occults a double star
  - Movie courtesy A. Bouchez
- Palomar 241-actuator adaptive optics system on the 5-m Hale telescope
- PHARO near-IR camera, K' filter (1.95 – 2.30 µm)

- Example laser occultation mission architecture
  - Movie courtesy A. Marinan
- Transmitting satellite in sun synchronous orbit, receiving satellite in ISS-deployed orbit
  - 2.26 mrad beamwidth
- Animation done with AGI STK software

Atmospheric Spectroscopy - Direct Imaging

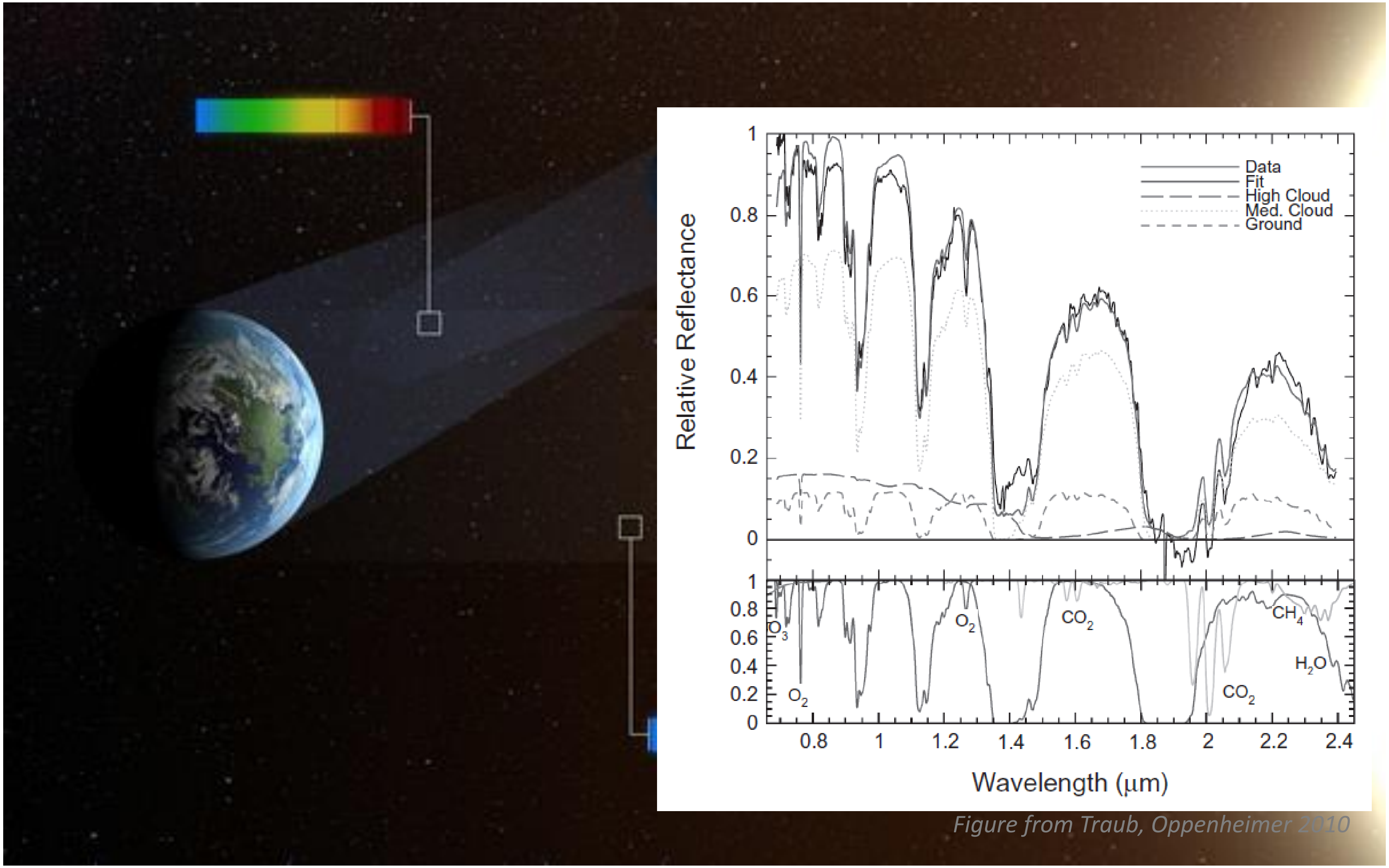

ESO/L. Calçada

MEMS Deformable Mirrors

- Actuators change the shape of the mirror surface to match the incoming wavefront
- MEMS devices
  - Electrostatic actuators
  - Stroke of ≈ 1 – 5 μm
  - High voltage, low current
  - More actuators
  - Less expensive
  - Fast response time
- Goal: use a CubeSat as a platform to demonstrate technology in space
  - Enable future earth and exoplanet characterization missions

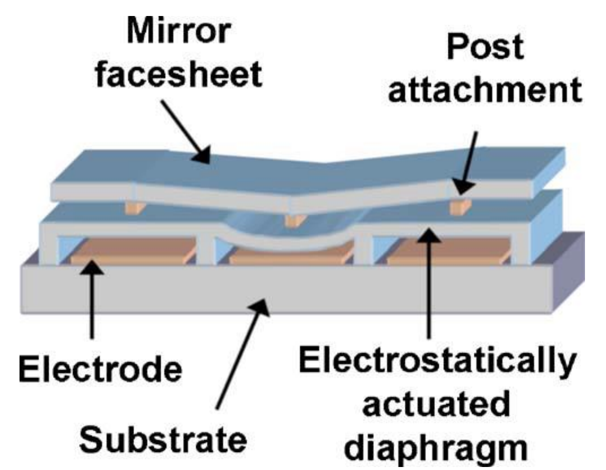

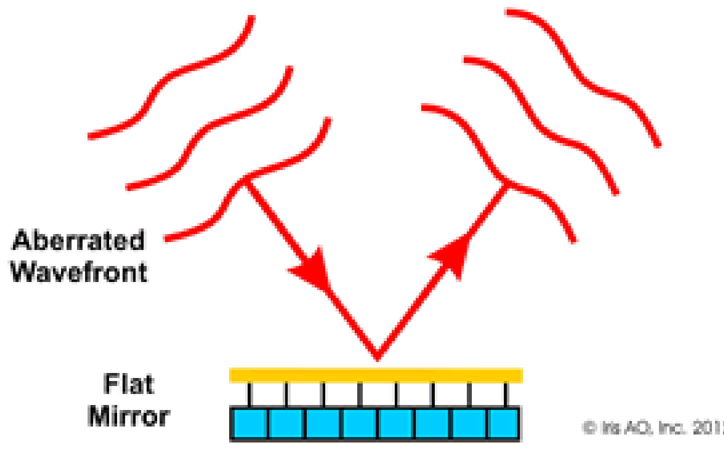

Stewart et al. 2007

Occultation with Lasers

- Intersatellite LEO IR laser link
  - Range of wavelengths from 2 – 2.5 um (other options possible)
- Transmitted signal is attenuated by atmosphere
  - Attenuation at different bands -> differential transmission -> thermodynamic variables composition information
- Transmitted signal also bent by atmosphere
  - Measure bending angle based on position of beam on detector (also requires knowledge of spacecraft position and altitude)

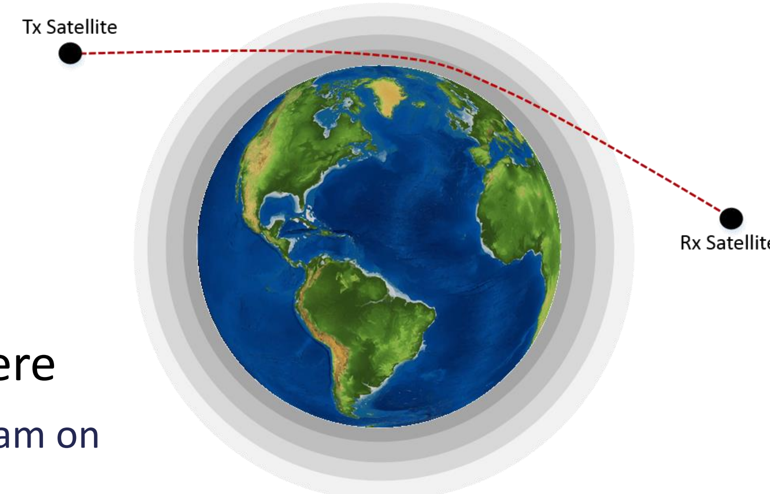

Marinan 2016

- Challenge:
  - Atmospheric turbulence induces its own aberration and attenuation
    - Messy point spread function - difficult to detect and centroid
  - **Solution: use wavefront control to improve signal measurements**
    - **Use nanosatellites for technology demonstrations of critical hardware (deformable mirrors)**

MEMS Deformable Mirrors in Space

- High spatial-frequency correction requires high actuator-density deformable mirrors
  - High Contrast Imaging: speckle nulling
  - Laser Communications and Intersatellite Links: atmospheric distortion
- Space Qualification – current/past efforts
  - MEMS Telescope for Extreme Lighting: Demonstration of MEMS mirror array on ISS
  - PICTURE and PICTURE-2: sounding rocket – observe exozodiacal dust
    - PICTURE-3: Balloon launch
  - NASA Ames ACE Lab – kilo MEMS deformable mirror in thermal vacuum testing
  - Technology Development for Exoplanet Missions: Boston Micromachines and Iris AO
    - T-Vac and vibration testing
    - Mirrors evaluated in coronagraph testbeds through Princeton and JPL
    - Qualify to survive launch environment (TRL ~6)

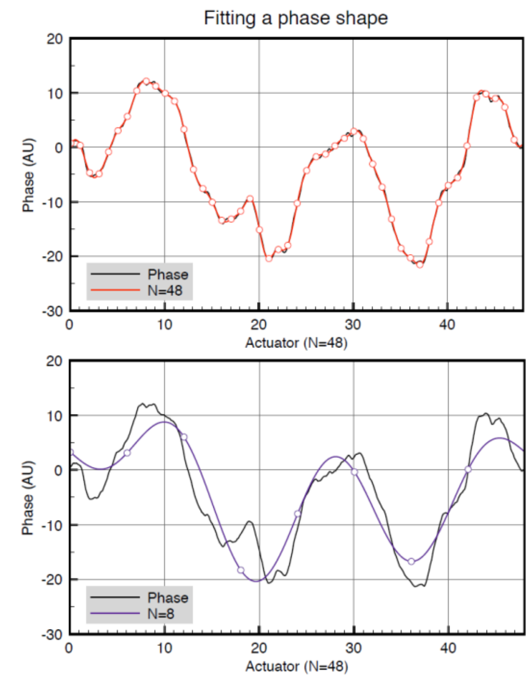

Image credit: L. Poyneer

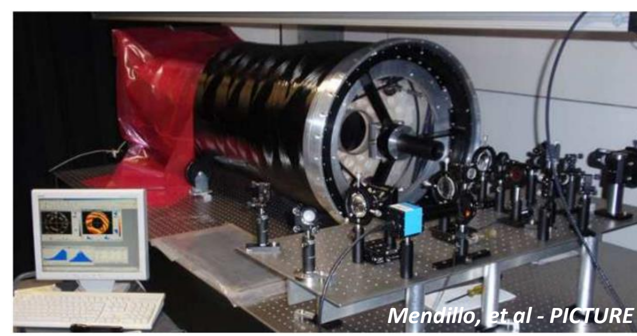

DeMi – Experiments

- Baseline orbit: ISS (~404x424 km)
- Target stars: Vega, Arcturis, Sirius, Canopis, Alpha Centauri
  - 5-8 minute orbit-averaged access opportunities

Experiment	Source	Sensor	Purpose	Operational Considerations
0	Internal Laser	Wavefront Sensor	Open and closed-loop mirror characterization	No payload-driven pointing requirements
1	Internal Laser	Focal Plane	Closed-loop wavefront sensing and correction demonstration	No payload-driven pointing requirements
2	External Object	Focal Plane	Closed-loop imaging, wavefront sensing and correction demonstration	Payload must track star and maintain stability over image exposure

0. Internal Source, S-H

<table>
<tr><th>Experiment</th><th>Description</th><th>Observables</th><th>Observable Performance</th><th>Success Criteria</th></tr>
<tr><td>Individual actuator pokes</td><td>Command each of 32 actuators in order to:
- 33% stroke
- 67% stroke
- 100% stroke</td><td rowspan="3">- X-Y displacement (in pixels) of spot after actuation

- Image of spots before and after actuation</td><td rowspan="3">- Maximum expected spot displacement: 1.5 µm stroke

- Minimum detectable spot displacement corresponding to 50 nm actuator motion</td><td rowspan="3">- Measured mirror deflection is within 100 nm rms of commanded deflection

- Mirror meets success criteria for 95% of all tests</td></tr>
<tr><td>Individual actuator pulls</td><td>Command all 32 actuators to 100% deflection. Command each of 32 actuators in order to:
- 67% stroke
- 33% stroke
- 0% stroke</td></tr>
<tr><td>Zernike surface maps</td><td>Command actuators to the following Zernike modes at 50% and 100%:
- Tip
- Tilt
- Defocus
- Astigmatism</td></tr>
</table>

1. Correct Image of Star (closed loop)

Experiment	Description	Observables	Observable Performance	Success Criteria
Correct static imperfections in optical system (Source: internal laser)	- Image focal plane and wavefront sensor with mirror unactuated - Apply closed-loop correction with wavefront sensor in the loop - Image focal plane and wavefront sensor with optimal mirror deflection	- Strehl before and after correction - Optimal commanded mirror voltage array for each parameter - Focal plane image before and after correction	- Mirror actuations of $\lambda/100$ rms detectable on focal plane - Strehl or encircled energy improves with each iteration	- Resulting Strehl >85% - Converge to correction within 8 minutes (TBR based on access times) - Actuators stay within 10%-90% stroke range

1. Correct Image of Star (closed loop)

Experiment	Description	Observables	Observable Performance	Success Criteria
Correct static imperfections in optical system (Source: external object)	- Image focal plane with mirror unactuated - Apply closed-loop correction with wavefront sensor in the loop - Image focal plane with optimal mirror deflection	- Focal plane image at beginning and end of observation - Strehl during observation	- Mirror actuations of λ/100 rms detectable on focal plane - Strehl or encircled energy improves with each iteration	- Resulting Strehl >80% - Converge to correction within 8 minutes (based on access times) - Actuators stay within 10%-90% stroke range

TRL 6 vs 7

- TRL 6:
  - System or subsystem model or prototype demonstrated in a relevant environment
  - A near final version of the technology in which additional design changes are likely is tested in real-life conditions.
- TRL 7
  - System prototype demonstrated in a relevant environment
  - The final prototype of the technology that is as close to the operational version as possible at this stage is tested in real-life conditions.

Wavefront Reconstruction

- Measure wavefront to determine shape of mirror
- Sensored – optical element introduced into beampath to generate measurement
- Sensorless – intensity-based measurements, computationally intensive

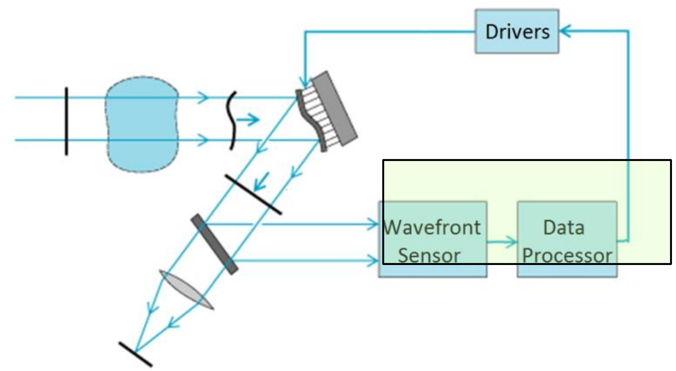

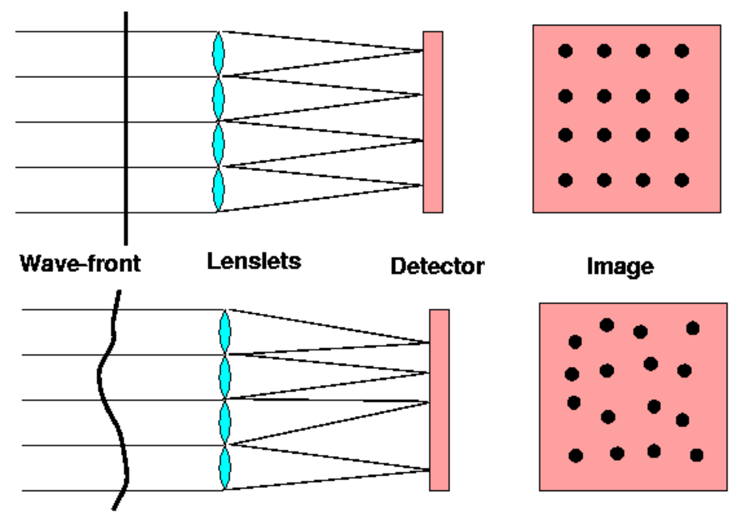

Shack Hartmann Design

- Driven by desired mirror stroke measurement and resolution

Parameter	Threshold	Units
Design wavelength	635	nm
Mirror Stroke	1.5	µm
Mirror Pitch	300	µm
Desired spot sampling	2.0	pixels/(λ/D)
Desired min detectable wavefront error	5.0	nm
Desired max detectable wavefront error	3.0	µm
Pixel pitch	5.2	µm
Lenslet pitch	300	µm
Lenslet focal length	4.8	mm
Actual max detectable wavefront error	8.8	µm
Centroid placement error for min detectable wavefront error	**0.02**	**pixels**

Focal Plane Sensor Design

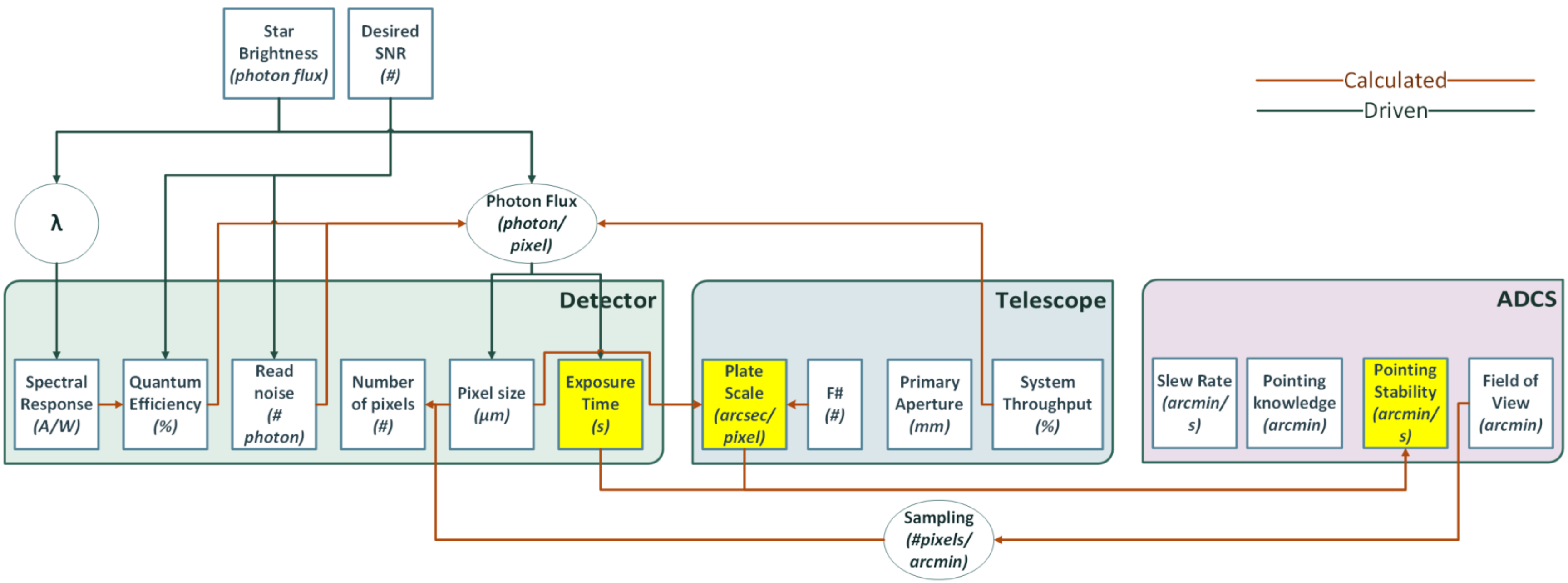

Focal Plane Sensor Design

- Driven by desire to image a star

Parameter	Threshold	Units
Aperture Diameter	0.0254	m
Telescope Effective Focal Length	0.4	m
Design wavelength	400-700	nm
System resolution (1.22 L/D)	5.4	arcsec
Telescope Field of View (width)	1.0 x 0.8	degrees
System throughput	47	%
Detector readout noise	5	photons/pixel
Detector dark noise	60	electrons/s
Detector quantum efficiency	55	%
Desired SNR at detector	10.0	--
Photoelectrons flux per pixel from star	5e6	photons/pixel/s
Required minimum exposure time	**0.001**	**seconds**

AO CubeSat Payload – Software

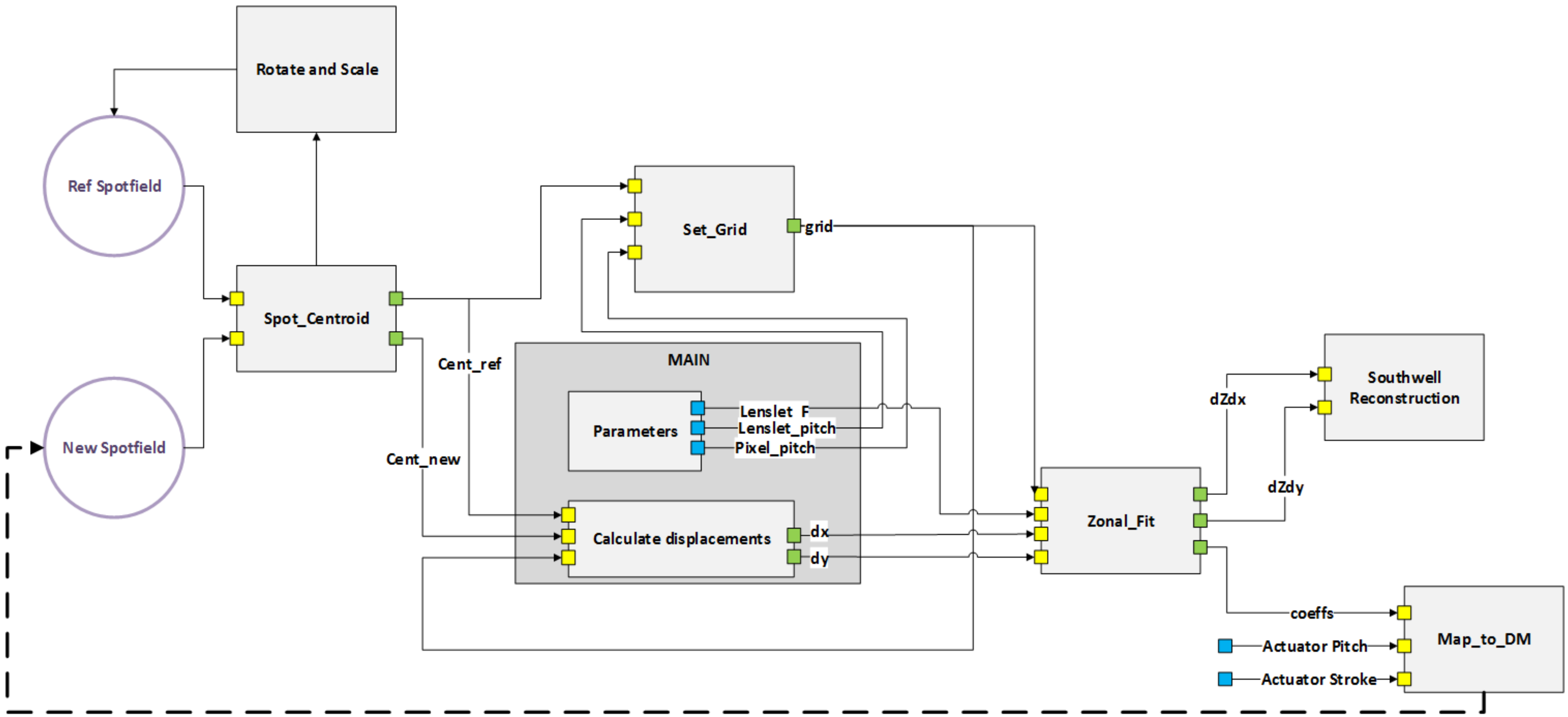

Wavefront Reconstruction Validation

- Reconstruction based on Southwell method
  - Average slopes from four surrounding lenslets (up, down, left, right)
- “Truth” Data
  - Zygo Interferometer (JPL)
  - Measurements at 20% stroke actuation

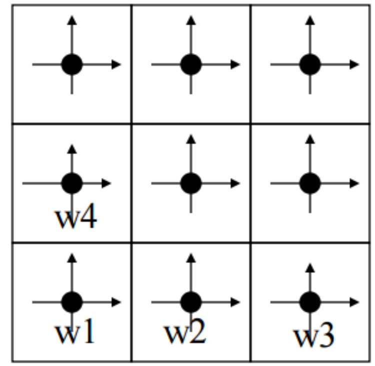

$$\frac{s_1^x + s_2^x}{2} = w_2 - w_1$$

$$\frac{s_1^y + s_4^y}{2} = w_4 - w_1$$

Southwell, 1980

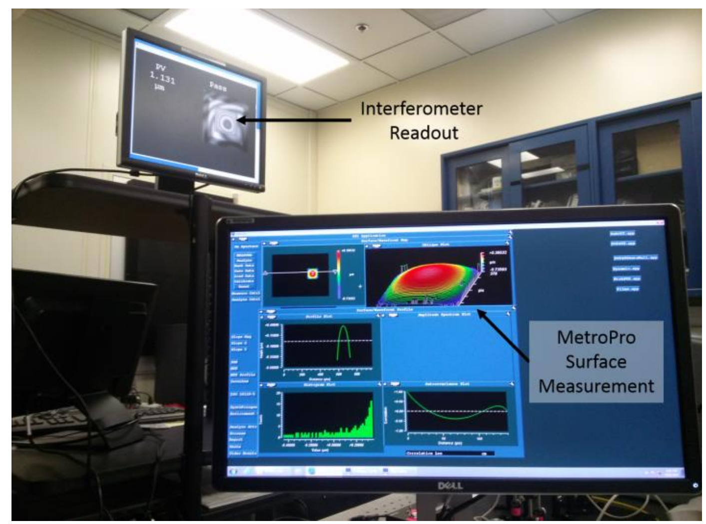

Zygo Interferometer Setup

Closed Loop Correction Validation

- Wavefront measurement converted from spot motion to "mirror space"
  - Interaction matrix – saved measurements of individual mirror pokes at maximum stroke
    - Assume linear scaling with actuator height
  - No open-loop reconstruction done within control algorithm
- Basic pseudo-inverse reconstructor
  - Piston subtraction and scaling: ensure that command to mirror is within mirror control authority
  - For more complex applications, can remove tip/tilt, create weighted matrix based on subaperture lighting, covariance matrix based on expected atmospheric variability

α = actuator
X = spot displacement in x
Y = spot displacement in y
M = number of actuators
N = number of subapertures

$$\begin{pmatrix} \alpha_{1x1} & \cdots & \alpha_{mx1} \\ \vdots & \ddots & \vdots \\ \alpha_{1yn} & \cdots & \alpha_{myn} \end{pmatrix}$$

$$Y = Ax$$

Observed spot motion (x and y)

Vector of actuator motion